



HAL
open science

Robust bounded control scheme for quadrotor vehicles under high dynamic disturbances

J. Betancourt, Pedro Castillo Garcia, P. García, V. Balaguer, Rogelio Lozano

► **To cite this version:**

J. Betancourt, Pedro Castillo Garcia, P. García, V. Balaguer, Rogelio Lozano. Robust bounded control scheme for quadrotor vehicles under high dynamic disturbances. *Autonomous Robots*, 2023, 47 (8), pp.1245-1254. 10.1007/s10514-023-10124-6 . hal-04345264

HAL Id: hal-04345264

<https://hal.science/hal-04345264>

Submitted on 14 Dec 2023

HAL is a multi-disciplinary open access archive for the deposit and dissemination of scientific research documents, whether they are published or not. The documents may come from teaching and research institutions in France or abroad, or from public or private research centers.

L'archive ouverte pluridisciplinaire **HAL**, est destinée au dépôt et à la diffusion de documents scientifiques de niveau recherche, publiés ou non, émanant des établissements d'enseignement et de recherche français ou étrangers, des laboratoires publics ou privés.

Robust bounded control scheme for quadrotor vehicles under high dynamic disturbances

J. Betancourt^{1*}, P. Castillo¹, P. García², V. Balaguer² and R. Lozano¹

¹*Heudiasyc (Heuristics and Diagnosis of Complex Systems), CS 60 319 - 60 203, Université de Technologie de Compiègne, 57 Av. de Landshut, Compiègne, 60200, France.

²Instituto Universitario de Automática e Informática Industrial (AI2), Universitat Politècnica de València (UPV), Camino de Vera S/n, Edificio 8G Acceso D planta 4, Valencia, 46022, Spain.

*Corresponding author(s). E-mail(s): gubetanc@hds.utc.fr.com;

Contributing authors: castillo@hds.utc.fr.com; pggil@isa.upv.es; vibagar3@upvnet.upv.es; rlozano@hds.utc.fr.com;

Abstract

In this paper, an optimal bounded robust control algorithm for secure autonomous navigation in quadcopter vehicles is proposed. The controller is developed combining two parts; one dedicated to stabilize the closed-loop system and the second one for dealing and estimating external disturbances as well unknown nonlinearities inherent to the real system's operations. For bounding the energy used by the system during a mission and, without losing its robustness properties, the quadratic problem formulation is used considering the actuators system constraints. The resulting optimal bounded control scheme improves considerably the stability and robustness of the closed-loop system and at the same time bounds the motor control inputs. The controller is validated in real-time flights and in unconventional conditions for high wind-gusts and LoE - Loss of Effectiveness- in two rotors. The experimental results demonstrate the good performance of the proposed controller in both scenarios.

Keywords: keyword1, Keyword2, Keyword3, Keyword4

1 Introduction

Quadcopters have been the most preferred multi-rotor aerial robot configuration for civilian applications [1, 2]. Due to their simplicity and versatility, quadcopters have attracted the attention of a large part of control and robotic scientific communities in front of other types of UAVs [3]. However, quadcopters have some disadvantages; for example, it is an underactuated system, unstable, with nonlinearities and fast dynamics as well

as couplings between their different loops. Nevertheless, these disadvantages represent a challenge for the control scientific community [4]. With the increasing demand of autonomous flights under different conditions, controlling a quadcopter stills an important challenge. For instance, the position and attitude controls of the quadcopter are extremely sensitive to external disturbances such as wind gusts [5]. Therefore, the design of robust regulators become more attractive for outdoor missions and practical applications.

In particular, robustness issues may be critical for quadcopter control since it can be subjected to undesired nonlinear dynamics and external disturbances. In order to weaken the effect of wind gusts, some authors have proposed complex control techniques to achieve stability. In [6–8] adaptive controllers with different structures were proposed and verified by simulations and experiments on test a bench. However, others researchers preferred to apply a Disturbance Observer Based Control (DOBC) strategy for attenuating external/internal disturbances. Among the most used DOBC techniques, it is worthy highlight the followings [9–11]. In these works, the Disturbance Observer (DOB) uses the transfer function of the system to compare the analytical desired performance with the real one and then, the difference between these inputs of these systems is taken as the disturbance. Despite several works found in the literature propose guaranteeing robustness of the system, few of them bounds the control inputs for limiting the energy applied in the system. This is because in some cases, bounding the control input only guarantees the robustness in a small range of external disturbances [12].

Bounding the control input is a challenge when implementing theoretical control results in real systems. This is due to the fact that, if the control signal exceeds the control inputs limits, it may lead to undesirable behavior of the system and therefore loose the stability. The anti-windup technique is frequently used in wide range of applications to solve this problem. For example, the analysis of the aircraft control system with input saturation conducted in [13] has shown existence of hidden oscillations, which were compensated by an anti-windup scheme. In [14] the anti-windup approach was proposed and then applied for the aircraft control problem in [15, 16]. This anti-windup algorithm was based on the property of convergence for marginally stable linear plants with saturated inputs. Furthermore, in [17] an iterative thrust-mixing scheme based on the LQR approach, to compute the desired single rotor thrusts and a prioritizing motor-saturation, was validated in real-time tests. In [18], a cascade integration of Incremental Nonlinear Dynamic Inversion (INDI) for the attitude and position control of micro aerial vehicles is addressed. Wind tunnel experiments show that the vehicle can enter and

leave the 10 *m/s* wind tunnel flow with only 21 cm maximum position deviation on average. In most of all these works, the desired collective thrust and body torques need to be converted into four single rotor thrusts. Consequently, it can be applied by means of the mapping from motors commands to rotor thrusts, i.e., *thrust mapping* [17].

For autonomous navigation, aerial vehicles need robust control systems to compensate the adverse effects produced by parametric and non-parametric uncertainties, unknown dynamics and atmospheric disturbances [19]. In flight real-time applications the robot is exposed to these undesired situations, therefore, the controller computes large amount of energy for counteracting them. Thus, if this energy is sent without a priori knowledge and during large periods of time, the actuators can be overheated and damaged leading to poor performance or undesirable crashes. This situation happens because they have physical constraints that often are not considered when computing the control law, e.g. maximum angular velocity in a motor.

In this work, we strive for a robust bounded control architecture by combining a nonlinear/linear controller and an uncertainty disturbances estimator. The idea behind of our approach is to bound the control input actuators while considering their constraints such that, the disturbance estimator is aware of these limits and therefore the disturbance compensation is as well bounded. This approach guarantees the robustness when dealing with undesired nonlinear dynamics and high dynamic disturbances. The proposed optimal bounded robust control architecture is depicted in Figure 2. The scheme is validated experimentally in real-time flights under unconventional conditions for high wind-gusts and LoE in two rotors. In addition, it is worth to highlight that even if our architecture does not use classical Fault Tolerant Control (FTC) schemes, it is capable to detect, estimate and compensate Loss of Effectiveness in rotors, fast enough, even when the aerial robot is flying in a non-hover position.

The rest of the paper is organized as follows: in Section 2, the dynamic model of quadrotor is recalled. The optimal bounded robust control scheme is addressed in Section 3. Experimental real-time tests to demonstrate the good performance of the proposed architecture, are provided

in Section 4. Finally, conclusion and future work are discussed in Section 5.

2 Problem formulation

The dynamic model of a quadcopter can be described by representing the vehicle as a 3D rigid body, which is driven by forces and torques generated by the propellers, see Fig 1. Therefore, the nonlinear model of the quadcopter using the Newton-Euler formalism can be expressed as [20]

$$\begin{aligned} \dot{\boldsymbol{\xi}}(t) &= \mathbf{v}(t), & m\ddot{\boldsymbol{\xi}}(t) &= \mathbf{R}(t)\mathbf{F}(t) - m\mathbf{g}\mathbf{e}_z, \\ \dot{\mathbf{R}}(t) &= \mathbf{R}(t)\hat{\boldsymbol{\Omega}}(t), & \mathbf{J}\dot{\boldsymbol{\Omega}} &= -\boldsymbol{\Omega}(t) \times \mathbf{J}\boldsymbol{\Omega}(t) + \boldsymbol{\tau}(t), \end{aligned} \quad (1)$$

where $\boldsymbol{\xi}(t)$ denotes the vector position of the vehicle with respect to the inertial frame \mathcal{I} , $\mathbf{v}(t) \in \mathcal{I}$ describes its linear velocity, $\boldsymbol{\Omega}(t)$ represents the angular velocity of the body defined in \mathcal{B} , and m is its total mass. The constant moment of inertia is \mathbf{J} expressed in \mathcal{B} , $\boldsymbol{\tau}(t) \triangleq [u_2, u_3, u_4]$ expresses the torques applied in the rigid body, $\hat{\boldsymbol{\Omega}}(t)$ introduces the skew-symmetric matrix of $\boldsymbol{\Omega}(t)$, $\mathbf{R}(t)$ means the rotation matrix from the body \mathcal{B} to the inertial \mathcal{I} frames, and $\mathbf{F}(t) \triangleq [0, 0, u_1]$ is the force vector applied to the robot.

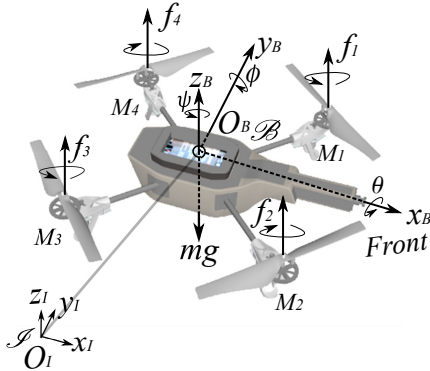


Fig. 1 Quadcopter aerial vehicle representation. $\mathcal{I} = \{x_I, y_I, z_I\}$ denotes the inertial frame, and $\mathcal{B} = \{x_B, y_B, z_B\}$ the body frame attached to center of mass of the vehicle. f_i expresses the force applied of motor i .

In this work, it is assumed that the thrust $f_i \approx k_f w_{M_i}^2$, and torque, $\tau_{M_i} \approx k_\tau w_{M_i}^2$, of each propeller are directly controlled by the angular rate of the motor, w_{M_i} , with k_f and k_τ are aerodynamic thrust and torque factors, respectively. Therefore,

from (1) and Figure 1, \mathbf{F} and $\boldsymbol{\tau}$ can be written as $\mathbf{F} = [0, 0, \sum_{i=1}^4 f_i]^T$ and $\boldsymbol{\tau} = [l(f_1 + f_4) - l(f_2 + f_3), l(f_1 + f_2) - l(f_3 + f_4), k_\tau(-f_1 + f_2 - f_3 + f_4)]^T$, with l representing the distance from the center of mass to the point where the force is applied.

Thus, the following relation for the control inputs can be established based on the angular rate of the rotors

$$\bar{\mathbf{u}} = \begin{bmatrix} u_1 \\ u_2 \\ u_3 \\ u_4 \end{bmatrix} = \begin{bmatrix} k_f & k_f & k_f & k_f \\ k_f l & -k_f l & -k_f l & k_f l \\ k_f l & k_f l & -k_f l & -k_f l \\ -k_\tau & k_\tau & -k_\tau & k_\tau \end{bmatrix} \begin{bmatrix} \omega_{M_1}^2 \\ \omega_{M_2}^2 \\ \omega_{M_3}^2 \\ \omega_{M_4}^2 \end{bmatrix}. \quad (2)$$

Bounding the controller without degrading the closed-loop system performance is a challenge, and several works have been proposed in the literature [21–26]. Nevertheless, most of them only consider the bound in the control laws without taking into account their actuators allocation. In this work, we propose an optimal bounded control algorithm for quadrotor aerial vehicles. The control law is composed by two parts; one dedicated to stabilize the vehicle when it is close to ideal conditions. The second one is capable to estimate and compensate the endogenous and exogenous properties of the system, such as undesired dynamics (produced by fault in motors) or external perturbations. In addition, the controller is developed to find the optimal values of the control law for avoiding saturate or overheat the actuators.

3 Optimal bounded robust control scheme

System (1) can be also expressed as a perturbed nonlinear system with the form

$$\dot{\mathbf{x}}(t) = \mathbf{A}\mathbf{x}(t) + \mathbf{B}\bar{\mathbf{u}}(t) + \mathbf{f}(\mathbf{x}, \bar{\mathbf{u}}, t) + \mathbf{d}(t) \quad (3)$$

where $\mathbf{A} \in \mathbb{R}^{n \times n}$ and $\mathbf{B} \in \mathbb{R}^{n \times m}$ are the system matrices, $\mathbf{x}(t) = [\boldsymbol{\xi}, \boldsymbol{\eta}]^T \in \mathbb{R}^n$ and $\bar{\mathbf{u}}(t) \in \mathbb{R}^m$ are the state and control vectors respectively, $\mathbf{f}(\mathbf{x}, \bar{\mathbf{u}}, t) : \mathbb{R}^n \times \mathbb{R} \times \mathbb{R}^+ \rightarrow \mathbb{R}^n$ defines an unknown non-linear function, and $\mathbf{d}(t) : \mathbb{R}^+ \rightarrow \mathbb{R}^n$ denotes the vector of unknown external disturbances. $\boldsymbol{\eta}$ represents the attitude vector of the vehicle, with $\boldsymbol{\Omega} = \mathbf{W}_\eta \dot{\boldsymbol{\eta}}$ and \mathbf{W}_η defines the standard kinematics relation between $\boldsymbol{\Omega}$ and $\boldsymbol{\eta}$. The full state is assumed to be measurable.

Assumption 1. The nonlinear function $\frac{\partial[\mathbf{f}(\mathbf{x}, \bar{\mathbf{u}}) + \mathbf{B}\bar{\mathbf{u}}]}{\partial \bar{\mathbf{u}}} \neq 0$, for all $(\mathbf{x}, \bar{\mathbf{u}}) \in \mathbb{R}^n \times \mathbb{R}^m$.

3.1 Control law

The goal is to regulate the state $\mathbf{x}(t)$ of the closed-loop system so that it asymptotically tracks the state of the reference model

$$\dot{\mathbf{x}}_q(t) = \mathbf{A}_q \mathbf{x}_q(t) + \mathbf{B}_q r_q(t), \quad (4)$$

where $\mathbf{x}_q \in \mathbb{R}^n$, $\mathbf{A}_q \in \mathbb{R}^{n \times n}$ and $\mathbf{B}_q \in \mathbb{R}^{n \times m}$ are the state vector, the state matrix and the control vector, respectively and \mathbf{A}_q a Hurwitz matrix.

The goal is that $\mathbf{x} \rightarrow \mathbf{x}_q$, therefore, the following error can be proposed

$$\mathbf{e} = (\boldsymbol{\xi} - \boldsymbol{\xi}_q, \boldsymbol{\eta} - \boldsymbol{\eta}_q)^\top = \mathbf{x} - \mathbf{x}_q. \quad (5)$$

Differentiating (5) and using (3), (4) such that adding and subtracting $\mathbf{A}_q \mathbf{x}$ it holds that

$$\dot{\mathbf{e}} = \mathbf{A}_q \mathbf{e} - \boldsymbol{\Gamma}, \quad (6)$$

with

$$\boldsymbol{\Gamma} = \mathbf{A} \mathbf{x} - \mathbf{A}_q \mathbf{x} - \mathbf{B}_q r_q + \mathbf{B} \bar{\mathbf{u}} + \mathbf{f}(\mathbf{x}, \bar{\mathbf{u}}, t) + \mathbf{d}(t)$$

Observe that if $\boldsymbol{\Gamma} \rightarrow 0$ then (6) will be asymptotically stable. Hence, $\bar{\mathbf{u}}$ can be proposed as

$$\bar{\mathbf{u}} = \mathbf{B}^+ \left[\underbrace{[(\mathbf{A}_q - \mathbf{A})\mathbf{x} + \mathbf{B}_q r_q]}_{\mathbf{u}_n} - \underbrace{[\mathbf{f}(\mathbf{x}, \bar{\mathbf{u}}, t) + \mathbf{d}(t)]}_{\mathbf{u}_\zeta} \right] \quad (7)$$

where $\mathbf{B}^+ = (\mathbf{B}^T \mathbf{B})^{-1} \mathbf{B}^T$ corresponds to the pseudo-inverse of \mathbf{B} . The first part of the proposed control law concerns to the reference tracking performance of the linear system (4). On the other hand, \mathbf{u}_ζ will contain the non-linear part of the controller. Then, the goal will be to compute \mathbf{u}_n and u_ζ . $\mathbf{u}_n = \mathbf{K} \mathbf{x}(t) + \mathbf{B}^+ \mathbf{B}_q r_q(t)$, with $\mathbf{K} = \mathbf{B}^+ (\mathbf{A}_q - \mathbf{A})$ representing the control part for stabilizing the system in ideal conditions.

In addition, observe that \mathbf{u}_ζ is a function of unknown variables, i.e., $\mathbf{u}_\zeta = \mathbf{f}(\mathbf{x}, \bar{\mathbf{u}}, t) + \mathbf{d}(t)$, and therefore it is difficult to estimate this parameter in this form. However, using (3), it can be

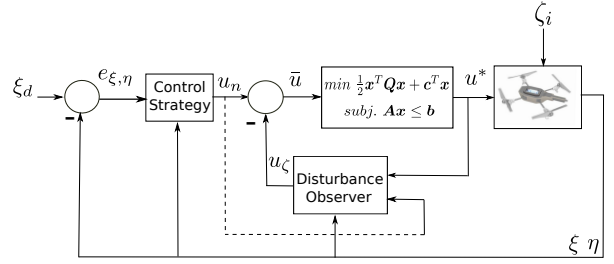


Fig. 2 Block diagram of the control structure. \mathbf{u}_n and \mathbf{u}_ζ correspond to the nominal control action and the control rejection part, respectively, ξ_d is the desired reference, ξ, η means the position and attitude states. $\bar{\mathbf{u}}$ and u^* represent the proposed controller and the set of its optimal and bounded values, respectively. The quadratic problem block deals with the motors constraints and ζ represents external disturbances.

rewritten as

$$\mathbf{u}_\zeta = \mathbf{B}^+ [\mathbf{A} \mathbf{x} + \mathbf{B} \bar{\mathbf{u}} - \dot{\mathbf{x}}]. \quad (8)$$

From (8), we can deduce that the unknown dynamics and disturbances can be estimated from the known dynamics of the systems and control signal.

Computing \mathbf{u}_ζ in the form (8) is not causal but \mathbf{u}_ζ will be implemented in a micro-controller. Hence for solving it, the Laplace transform is applied. Then, (8) becomes

$$\mathbf{u}_\zeta(s) = \mathbf{G}_f(s) \mathbf{B}^+ [\mathbf{A} \mathbf{x}(s) + \mathbf{B} \bar{\mathbf{u}}(s) - s \mathbf{x}(s)], \quad (9)$$

where $\mathbf{G}_f(s)$ is a strictly proper stable low-pass filter with unity gain and zero phase shift over the spectrum of the uncertain term $\mathbf{f}(\mathbf{x}, \bar{\mathbf{u}}, t) + \mathbf{d}(t)$ [27].

3.2 Bounded observer

In quadrotor systems the real control inputs are related with the energy computed by the motors using the relation of the control inputs $\bar{\mathbf{u}}$, as can be stated in (2), for obtaining the angular velocities of each motor. This relation is often obtained when the control laws $\bar{\mathbf{u}}$ need to be transformed into the real control inputs, i.e., the actuators (motors). For the quadrotor vehicle it can be expressed as

$$\mathbf{M} = \mathbf{H} \bar{\mathbf{u}}, \quad (10)$$

with

$$\mathbf{M} = \begin{bmatrix} M_1(t) \\ M_2(t) \\ M_3(t) \\ M_4(t) \end{bmatrix}; \quad \bar{\mathbf{u}} = \begin{bmatrix} u_1(t) \\ u_2(t) \\ u_3(t) \\ u_4(t) \end{bmatrix} = \begin{bmatrix} u_{n_1} + u_{\zeta_1} \\ u_{n_2} + u_{\zeta_2} \\ u_{n_3} + u_{\zeta_3} \\ u_{n_4} + u_{\zeta_4} \end{bmatrix};$$

and \mathbf{H} denotes the allocation control matrix with the form

$$\mathbf{H} = \begin{bmatrix} 1 & 1 & 1 & -1 \\ 1 & -1 & 1 & 1 \\ 1 & -1 & -1 & -1 \\ 1 & 1 & -1 & 1 \end{bmatrix}$$

Notice that (10) represents the real robust control input applied to the i -th actuator (M_i) for controlling the aerial vehicle. If the vehicle is affected by external disturbances or undesired dynamics, the controller needs to be capable to estimate and compensate them. However, when the quadrotor is dealing with aggressive and constant perturbations or repetitive missions (tests), the motors can be overheated in several cases, resulting in a physical damage or degradation on its performance. For avoiding that, it is necessary to compute a set of the optimal bounded control inputs, \mathbf{u}^* , from $\bar{\mathbf{u}}$.

Hence, \mathbf{u}^* can be obtained as

$$\mathbf{u}^* = \delta_M^T \bar{\mathbf{u}}, \quad (11)$$

where $\delta_M^T = [\delta_1 \ \delta_2 \ \delta_3 \ \delta_4]$ with δ_i defining a factor for fulfilling the rotors constraints. The bounds for the motors control inputs can be found solving the following quadratic problem

$$\min_{\delta_M} \frac{1}{2} \delta_M^T \mathbf{Q} \delta_M + \mathbf{c}^T \delta_M \quad (12)$$

$$st. \ \mathbf{A}_M \delta_M \leq \mathbf{b}, \quad (13)$$

where \mathbf{Q} , \mathbf{c} , \mathbf{A}_M , \mathbf{b} are matrices and vectors that will be defined later.

For computing matrices and vectors in (12) and (13), the following cost-to-go function can be defined as

$$f_o = \sum_{i=1}^4 Q_i (\bar{u}_i - u_i^*)^2, \quad (14)$$

where Q_i is a weight value penalizing the control input. Developing the above equation, it follows

that

$$f_o = \sum_{i=1}^4 Q_i (\bar{u}_i^2 - 2\delta_i \bar{u}_i^2 + \delta_i^2 \bar{u}_i^2). \quad (15)$$

From (15), note that the term \bar{u}_i^2 does not affect to find the minimum of the quadratic problem, thus, it can be neglected. Rewriting the above equation in matrix form, it yields

$$f_o = \frac{1}{2} \delta_M^T \mathbf{Q} \delta_M + \mathbf{c}^T \delta_M,$$

with

$$\mathbf{Q} = \begin{bmatrix} Q_1 \bar{u}_1^2 & 0 & 0 & 0 \\ 0 & Q_2 \bar{u}_2^2 & 0 & 0 \\ 0 & 0 & Q_3 \bar{u}_3^2 & 0 \\ 0 & 0 & 0 & Q_4 \bar{u}_4^2 \end{bmatrix}, \quad \mathbf{c} = \begin{bmatrix} -Q_1 \bar{u}_1^2 \\ -Q_2 \bar{u}_2^2 \\ -Q_3 \bar{u}_3^2 \\ -Q_4 \bar{u}_4^2 \end{bmatrix}.$$

Let us introduce the constraints on the motors control inputs with the form $\sigma_i \leq M_i \leq \bar{\sigma}_i$, where $\bar{\sigma}_i$ and σ_i are the upper and lower bounds of the motors, respectively. Moreover, define u_0^* as the equilibrium point of the aerial robot at hover position, in other words, the u_1 needed to compensate the weight of the vehicle.

For finding condition (13), consider the case of the motor $M_1 \leq |\sigma_1|$. Thus, taking into account the weight compensation u_0^* and using (10) with the optimal value of $\bar{\mathbf{u}}$ (11), it follows that

$$|\delta_1| |\bar{u}_1| + |\delta_2| |\bar{u}_2| + |\delta_3| |\bar{u}_3| - |\delta_4| |\bar{u}_4| \leq |\sigma_1| - u_0^*. \quad (16)$$

Then, following the same procedure for the rest of motors but considering the general form

$$\left| \sum_{i=1}^4 \pm \delta_i \bar{u}_i \right| \leq |\bar{\sigma}_i| - u_0^* \quad (17)$$

and rewriting them in a matrix form, it follows that (13) is founded with

$$\mathbf{A}_M = \begin{bmatrix} +\bar{u}_1 + \bar{u}_2 + \bar{u}_3 - \bar{u}_4 \\ +\bar{u}_1 - \bar{u}_2 + \bar{u}_3 + \bar{u}_4 \\ +\bar{u}_1 - \bar{u}_2 - \bar{u}_3 - \bar{u}_4 \\ +\bar{u}_1 + \bar{u}_2 - \bar{u}_3 + \bar{u}_4 \\ -\bar{u}_1 - \bar{u}_2 - \bar{u}_3 + \bar{u}_4 \\ -\bar{u}_1 + \bar{u}_2 - \bar{u}_3 - \bar{u}_4 \\ -\bar{u}_1 + \bar{u}_2 + \bar{u}_3 + \bar{u}_4 \\ -\bar{u}_1 - \bar{u}_2 + \bar{u}_3 - \bar{u}_4 \end{bmatrix}, \quad \mathbf{b} = \begin{bmatrix} \bar{\sigma}_1 - u_0^* \\ \bar{\sigma}_2 - u_0^* \\ \bar{\sigma}_3 - u_0^* \\ \bar{\sigma}_4 - u_0^* \\ -\sigma_1 + u_0^* \\ -\sigma_2 + u_0^* \\ -\sigma_3 + u_0^* \\ -\sigma_4 + u_0^* \end{bmatrix}.$$

Thus using (11) with constraints (12) and (13), it is possible to find the set of optimal bounded values of $\bar{\mathbf{u}}$. Then, (8) becomes

$$\mathbf{u}_\zeta(s) = \mathbf{G}_f(s) \mathbf{B}^+ [\mathbf{A} \mathbf{x}(s) + \mathbf{B} \mathbf{u}^*(s) - s \mathbf{x}(s)] \quad (18)$$

with $G_f(s) = \frac{1}{T_f s + 1}$, and $T_f > T$, being T the sample-time.

4 Experimental results

The practical goal of these experiments is to validate the proposed control architecture. For better illustrate the good performance of the optimal bounded robust controller (11), it is compared, in two scenarios, with respect to its nominal form (7). It is worth to mention that both algorithms have a low computational cost, which permits to be implemented in low cost CPU. The experimental tests are performed in a quadcopter vehicle AR Drone 2. Its firmware was modified to work under the software FI-AIR - Framework libre AIR which is open source and runs a Linux-based operating system, capable of implementing a wide range of control schemes, see [28]. An OptiTrack motion capture system was used to estimate the vehicle's position, while its internal Inertial Measurement Unit (IMU) measures its orientation and angular rates. A video of the experimental results can be seen in <https://youtu.be/El7xDcuCas8>

The control parameters are presented in the Table 1. Here, \bar{K}_{1_i} , \bar{K}_{2_i} , express the gains of the controller \mathbf{u}_n for each subsystem, $i : \phi, \theta, \psi, x, y, z$. Each state in (4) can be considered decoupled and modeled by a double integrator with the form $G(s) = b/s^2$ such that b can be obtained experimentally for each state. For control implementation the following low-pass filter $G_f = 1/(Ts + 1)$ is used, with T representing its bandwidth.

Table 1 Gain parameters used in the experimental tests

Parameter	ϕ, θ	ψ	x, y	z
\bar{K}_{1_i}	0.8	0.6	0.17	0.3
\bar{K}_{2_i}	0.1	0.2	0.13	0.1
b	140	44	10	5
T	0.1	0.5	0.5	0.3

4.1 First scenario: Aggressive wind-gust

Most of the aerial robot applications are developed in outdoors environments where robustness with respect to wind is a primary task. The goal of the first scenario is to show the performance of the quadcopter while it is at hover, subject to aggressive constant and intermittent wind-gust. For this

end, a leaf blower *Bosch AVS1* was used to emulate external wind gust with an airflow speed of 60km/h and placed at 1.5m from the quadrotor. The hover position is at: $x(0) = 0$, $y(0) = 0$, $z(0) = 1$ all in meters. A video of the experimental results can be seen in <https://youtu.be/0SrbkVlmUg>.

In Figure 3-up the performance of the vehicle in 3D space subject to high wind-gust is introduced. Notice the better performance of the optimal bounded robust controller \mathbf{u}^* with respect to $\bar{\mathbf{u}}$. The position behavior of the drone is depicted in Figure 3-down. In the experiment the wind-gust was directed to the y -axis the firsts 20s. Note that both approaches suffer a degradation in their performance, nevertheless it is clear that when using \mathbf{u}^* , this degradation (especially in z) is smoother.

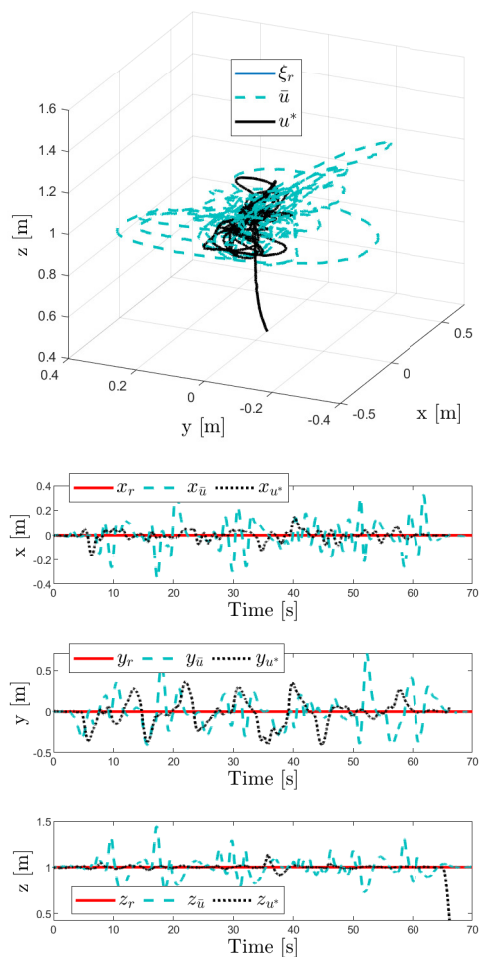


Fig. 3 Scenario 1.- System performance during flight tests.

Figure 4 depicts the performance of the disturbance estimations and the motors control input. Notice the relation between these figures. When the disturbance estimation is computed in the controller for compensating these undesired dynamics, notice that the nominal controller $\bar{\mathbf{u}}$, computes higher values exceeding the limits constraints in actuators (in our case is 1). However, when the vehicle is controlled by \mathbf{u}^* , observe that the aforementioned problem does not appears.

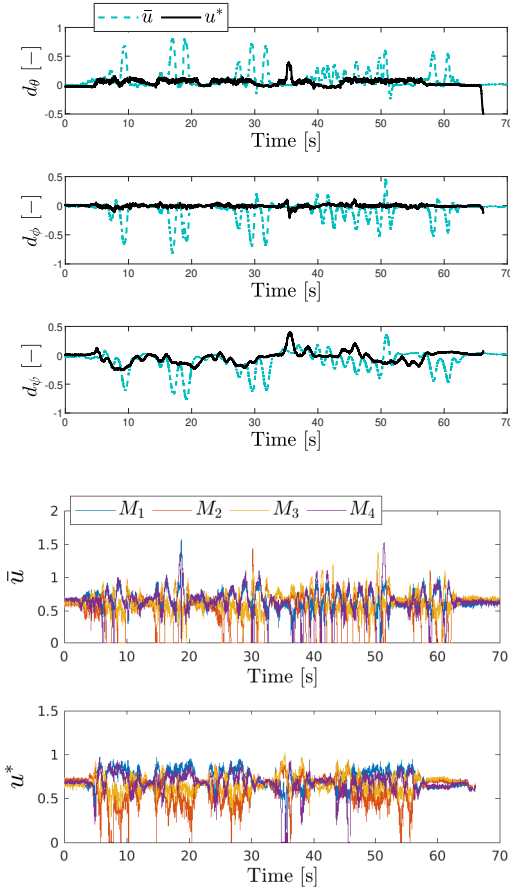


Fig. 4 Scenario 1.- Attitude disturbance estimation and motor control action performances.

4.2 Second scenario: Loss of effectiveness in rotors when performing a trajectory

Conducting electrical inspections with drones has been an application developed through the last years. In this kind of tasks, the vehicle needs to be

robust with respect to many factors, as wind-gust, possible loss of effectiveness in rotors (repetitive tasks), among others.

The goal of the second scenario is to show the performance of the quadcopter when two LoE in motors M_1 and M_2 occur while performing a desired trajectory emulating conduct electrical inspection. In this experiment, the efficiency in M_1 is reduced 40% at time $t \sim 28$ s and, later, at time $t \sim 44$ s, the efficiency in M_2 is reduced 20%. An helical trajectory with the form $x_r(t) = t$, $y_r(t) = a \sin(t)$ and $z_r(t) = a \cos(t)$ was chosen as desired trajectory, where a indicating the radius of the circumference. The initial conditions are defined as $\xi_r(0) = [-1, 1, 2]^T$ in meters. A video of this experiment can be seen at <https://youtu.be/rp0u8eeerh0>.

Figures 5- 6 show the performance of the quadcopter, while tracking the helical trajectory subject to LoE in two rotors. The behavior of the vehicle in 3D space is presented in Figure 5. Notice from this figure that when the first LoE (40%) in rotor M_1 was injected, the practical stability, when using $\bar{\mathbf{u}}$, is compromised making the drone becomes perturbed. Moreover, this controller was not capable to assure the stability of the system and therefore, it was not possible to apply the second LoE in rotor M_2 because the aerial robot crashed. Nevertheless, when using \mathbf{u}^* , the quadcopter can continue tracking the desired reference and even tough, compensate a second LoE (20%) in rotor M_2 at time $t \sim 44$ s.

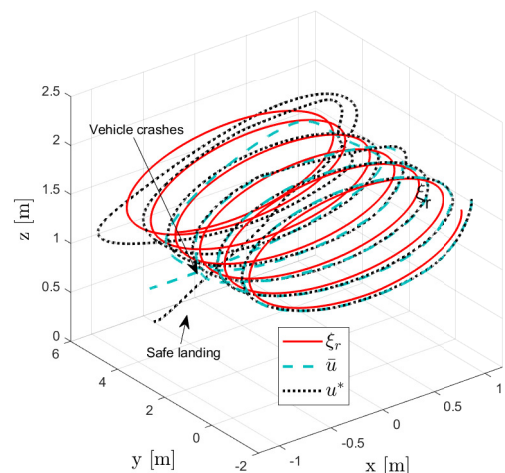


Fig. 5 Scenario 2.- 3D state performances in flight tests.

Figure 6 introduces the behavior of the disturbance estimation and the motor control inputs. Observe from these figures that when using \mathbf{u}^* , the vehicle suffers a small degradation on their performance without exceeding the physical constraints of the motors and even tough, it can overcome the second LoE around $t \sim 44\text{s}$ allowing to continue tracking the desired reference and landing safely.

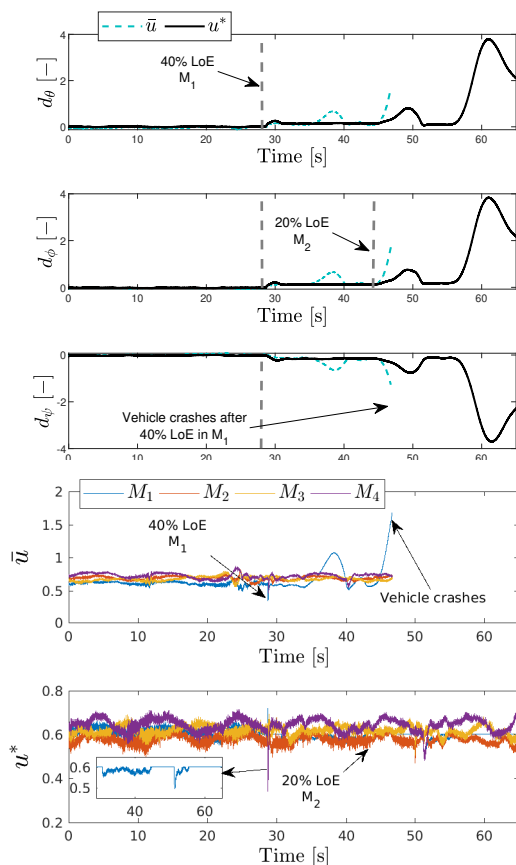


Fig. 6 Scenario 2.- Attitude disturbance estimation and motor control action performances.

5 Conclusions

An optimal bounded robust control algorithm was developed in this paper. This controller was conceived to be robust with respect to uncertain dynamics and external and unknown perturbations. Its structure contains two parts, one for stabilizing the aerial vehicle close to the ideal conditions (small angles) and the second one for estimating and compensating unknowns dynamics.

For improving robustness and avoiding saturate actuators in the system, the resulted controller of this scheme was bounded solving a quadratic problem in the control inputs and taken into account the motors constraints.

The proposed architecture was proved, in practice, when several wind-gust were applied while the vehicle was at hover. In addition, the scheme was also validated when loss of effectiveness (LoE) in rotors appears. Here, the practical goal was to track a desired trajectory while two LoE (one of 40% and the second of 20%) in two different motors were applied. Practical validations demonstrated the good performance of the proposed optimal bounded robust controller. Future work includes practical validation of the algorithm in different aggressive scenarios.

Acknowledgments. This work was supported by CONACyT - Mexico, the program Robotex Equipment of Excellence (ANR-10-EQPX-44) - France. The supports are gratefully acknowledged.

Declarations

- **Conflict of interest** The authors declare that they have no conflict of interest.
- **Funding** The funding was provided by the CONACyT- Mexico and the program Robotex Equipment of Excellence (ANR-10-EQPX-44).
- **Authors' contributions** All authors contributed equally to this work.

References

- [1] Amin, R., Aijun, L. & Shamshirband, S. A review of quadrotor UAV: control methodologies and performance evaluation. *International Journal of Automation and Control* **10** (2), 87–103 (2016) .
- [2] Tofigh, M. A., Mahjoob, M. J. & Ayati, M. Dynamic modeling and nonlinear tracking control of a novel modified quadrotor. *International Journal of Robust and Nonlinear Control* **28** (2), 552–567 (2018) .

- [3] Shraim, H., Awada, A. & Youness, R. A survey on quadrotors: Configurations, modeling and identification, control, collision avoidance, fault diagnosis and tolerant control. *IEEE Aerospace and Electronic Systems Magazine* **33** (7), 14–33 (2018) .
- [4] Saeed, A. S. *et al.* A review on the platform design, dynamic modeling and control of hybrid uavs. *2015 International Conference on Unmanned Aircraft Systems (ICUAS)* 806–815 (2015) .
- [5] Qian, L. & Liu, H. H. Path-following control of a quadrotor uav with a cable-suspended payload under wind disturbances. *IEEE Transactions on Industrial Electronics* **67** (3), 2021–2029 (2020). <https://doi.org/10.1109/TIE.2019.2905811> .
- [6] Yang, S., Han, J., Xia, L. & Chen, Y.-H. Adaptive robust servo constraint tracking control for an underactuated quadrotor uav with mismatched uncertainties. *ISA Transactions* **106**, 12–30 (2020) .
- [7] Jin, X.-Z., He, T., Wu, X.-M., Wang, H. & Chi, J. Robust adaptive neural network-based compensation control of a class of quadrotor aircrafts. *Journal of the Franklin Institute* **357** (17), 12241–12263 (2020) .
- [8] Labbadi, M. & Cherkaoui, M. Robust adaptive nonsingular fast terminal sliding-mode tracking control for an uncertain quadrotor uav subjected to disturbances. *ISA Transactions* **99**, 290 – 304 (2020) .
- [9] Guo, B.-Z. & liang Zhao, Z. On the convergence of an extended state observer for nonlinear systems with uncertainty. *Systems & Control Letters* **60** (6), 420–430 (2011) .
- [10] Huang, Y. & Xue, W. Active disturbance rejection control: Methodology and theoretical analysis. *ISA Transactions* **53** (4), 963–976 (2014). Disturbance Estimation and Mitigation .
- [11] Chen, W.-H. Disturbance observer based control for nonlinear systems. *IEEE/ASME Transactions on Mechatronics* **9** (4), 706–710 (2004) .
- [12] Narendra, K. & Annaswamy, A. Robust adaptive control in the presence of bounded disturbances. *IEEE Transactions on Automatic Control* **31** (4), 306–315 (1986) .
- [13] Andrievsky, B., Kuznetsov, N., Leonov, G. & Pogromsky, A. Hidden oscillations in aircraft flight control system with input saturation. *IFAC Proceedings Volumes* **46** (12), 75 – 79 (2013). 5th IFAC Workshop on Periodic Control Systems .
- [14] van den Berg, R., Pogromsky, A. & Rooda, K. Convergent systems design: Anti-windup for marginally stable plants. *Proceedings of the 45th IEEE Conference on Decision and Control* (6), 5441–5446 (2006). <https://doi.org/10.1109/CDC.2006.377054> .
- [15] Andrievsky, B. R., Kuznetsov, N. V., Leonov, G. A. & Pogromsky, A. Y. Convergence based anti-windup design method and its application to flight control. *2012 IV International Congress on Ultra Modern Telecommunications and Control Systems* 212–218 (2012) .
- [16] Leonov, G., Andrievsky, B., Kuznetsov, N. & Pogromskii, A. Aircraft control with anti-windup compensation. *Differential Equations* **48**, 1700–1720 (2012) .
- [17] Faessler, M., Falanga, D. & Scaramuzza, D. Thrust mixing, saturation, and body-rate control for accurate aggressive quadrotor flight. *IEEE Robotics and Automation Letters* **2** (2), 476–482 (2017) .
- [18] Smeur, E., de Croon, G. & Chu, Q. Cascaded incremental nonlinear dynamic inversion for mav disturbance rejection. *Control Engineering Practice* **73**, 79–90 (2018) .
- [19] Luque-Vega, L., Castillo-Toledo, B. & Loukianov, A. G. Robust block second order sliding mode control for a quadrotor. *Journal of the Franklin Institute* **349** (2), 719 – 739 (2012) .

- [20] Castillo, P., Lozano, R. & Dzul López, A. E. *Modelling and Control of Mini-Flying Machines* (Springer London, 2005).
- [21] Sun, L., Huo, W. & Jiao, Z. Adaptive backstepping control of spacecraft rendezvous and proximity operations with input saturation and full-state constraint. *IEEE Transactions on Industrial Electronics* **64** (1), 480–492 (2017) .
- [22] Cabecinhas, D., Cunha, R. & Silvestre, C. Saturated output feedback control of a quadrotor aircraft. *2012 American Control Conference (ACC)* 4667–4602 (2012) .
- [23] Li, S., Wang, Y. & Tan, J. Adaptive and robust control of quadrotor aircrafts with input saturation. *Nonlinear Dynamics* **89** (2017) .
- [24] Wang, Y., Ren, B., Zhong, Q.-C. & Dai, J. Bounded integral controller with limited control power for nonlinear multiple-input multiple-output systems. *IEEE Transactions on Control Systems Technology* **29** (3), 1348–1355 (2021) .
- [25] Gruszka, A., Malisoff, M. & Mazenc, F. Bounded tracking controllers and robustness analysis for uavs. *IEEE Transactions on Automatic Control* **58** (1), 180–187 (2013). <https://doi.org/10.1109/TAC.2012.2203056> .
- [26] Konstantopoulos, G. C., Zhong, Q.-C., Ren, B. & Krstic, M. Bounded integral control of input-to-state practically stable nonlinear systems to guarantee closed-loop stability. *IEEE Transactions on Automatic Control* **61** (12), 4196–4202 (2016) .
- [27] Zhong, Q.-C. & Rees, D. Control of uncertain lti systems based on an uncertainty and disturbance estimator. *Journal of Dynamic Systems, Measurement, and Control-Transactions of the ASME* **126** (4), 905–910 (2004) .
- [28] Lab, H. Fl-air - framework libre air (2012). <https://devel.hds.utc.fr/software/flair>, Sidst set 27/06/2021.